2018

The Role of Wave Self-Similarity in Nearshore Wave Spectra

Morgan M. Smith Mr.
University of North Florida, N00687625@unf.edu

THE ROLE OF WAVE SELF-SIMILARITY IN NEARSHORE WAVE SPECTRA

by

Morgan Smith, B.S.

A Thesis submitted to the Department of Civil Engineering

in partial fulfillment of the requirements for the degree of

Master of Science in Civil Engineering

UNIVERSITY OF NORTH FLORIDA

COLLEGE OF COMPUTING, ENGINEERING AND CONSTRUCTION

May 2018

The Thesis titled ***The Role of Self-Similarity of Nearshore Wave Spectra*** submitted by ***Morgan Menzies Smith*** in partial fulfillment of the requirements for the degree of Master of Science in Civil Engineering has been:

Approved by the thesis committee: **Date:**

Don T. Resio, Committee Chair

Dr. Thobias Sando, PhD

Dr. William Dally, PhD, PE

Accepted for the School of Engineering:

Dr. Murat Tiryakioglu, PhD, CQE
Director of the School of Engineering

Accepted for the College of Computing, Engineering, and Construction:

Dr. Mark Tumeo, PhD, PE
Dean of the College of Computing, Engineering, and Construction

Accepted for the University:

Dr. John Kantner, PhD
Dean of the Graduate School

ACKNOWLEDGEMENTS

I would like to thank my committee chair and thesis advisor Dr. Resio. The knowledge and assistance he has provided me with through graduate school is remarkable. I was very fortunate to have his help and guidance as a mentor. Also, I would to thank Dr. Dally and Dr. Sando for agreeing to be on my master's thesis committee and providing me support throughout the semesters I attended graduate school at the University of North Florida.

In addition, I would like to thank my parents. Without their support, I would not be the person I am today. My parents provided me with encouragement which enabled myself to push my education to the next level.

TABLE OF CONTENTS

LIST OF TABLES

LIST OF FIGURES

ABSTRACT

Nonlinear wave-wave interactions and wave breaking contribute to nearshore wave energy dissipation. These factors can be analyzed by the principles of wave self-similarity. The equilibrium range can be shown in wind-driven wave spectra that exist in the f^{-5} form (k^{-3}) and f^{-4} $\left(k^{-5/2} \right)$. However, the appropriate methods used to determine this loss of energy are controversial. This study examines an approach that reinvestigates the self-similarity principles. Wave spectra with lower peak periods are dominated by nonlinear wave-wave interactions which produce a $k^{-5/2}$ scaling in shallow water. This thesis investigates the relative role of spectral similarity in different conditions in the nearshore region of the U.S. Army Corps of Engineers Field Research Facility in Duck, North Carolina. The results show young sea waves (wave spectra in which the propagation speed of waves at the spectral peak is much smaller than the wind speed) are dominated by nonlinear wave-wave interactions in the nearshore while older waves (wave spectra in which the propagation speed of waves at the spectral peak is equal to or greater than the wind speed) are dominated by wave breaking in deep water. Furthermore, nearshore wave models need to incorporate the self-similarity concept in deep and shallow water to better understand and quantify important aspects of wave physics in shallow water.

CHAPTER 1: INTRODUCTION

The attenuation of wave energy has been a topic of extreme interest in coastal engineering for many decades now. Wave growth and decay are still not easily understood in shallow waters. Waves often lose much of their energy as they approach the coastline. Theoretical concepts for coastal energy dissipation include many different processes such as white capping, viscous attenuation, air resistance, nonlinear wave-wave interactions, and bottom friction. Understanding why and how waves dissipate is significant for many reasons that include analyzing coastal processes and coastal structures. For example, wave erosion is one of the primary factors attributing to beach morphology. Accurate predictions of erosion require accurate methods for estimating wave energy loss in nearshore areas. Researchers and scientists have followed different paths to develop applicable theories, and no consensus exists today. This thesis, examines the role of self-similarity in nearshore wind-generated waves in the context of two different energy loss mechanisms, wave breaking and nonlinear wave-wave interactions.

Understanding nearshore wave conditions is important for many aspects of coastal engineering. Today's state of the art, third-generation models, use optimized empirical source/sink terms, often with several free parameters to represent this process. For example, Alves and Banner (2001) derive a single dissipation source term (wave breaking) that contains several free parameters which all had to be optimized to fit a given data set. Source-term parameterizations in shallow-water utilize even more empirical functions which must each be tuned to approximate wave transformations in a specific area. On the other hand, the theory of a process-based equilibrium range in wind-generated waves presented by Phillips (1958) suggested a simpler approach, that energy distributions in wave spectra could be analyzed using dimensionally-based similarity principles. Bouws et al. (1985) incorporated the Texel, Marsen, and Arsloe Spectrum (TMA Spectrum) into analyses to describe a self-similar spectral shape to describe wind waves in water of finite depth. With the TMA Spectrum, the specification of a generalized shallow-water form developed, retaining the fundamental f^{-5} form, was transformed to an "arbitrary-depth"

wavenumber basis utilizing a wavenumber basis in place of frequency. This theory was applied to the JONSWAP Spectrum (Hasselmann et al., 1973). Analyzing wave spectra in wavenumber space evaluates the scaling across the entire spectrum and suggested that a single dominant mechanism controls the entire spectral shape (Bouws et al., 1985).

Bouws et al. (1985) transformed deep-water spectra into wavenumber space and assumed that the variation in the dispersion relationship would apply to arbitrary depths, under the assumption that the general mechanism controlling the spectral shape is wave breaking following the similarity arguments presented by Kitaigorodskii (1975). Subsequently, mounting observational evidence that equilibrium ranges in deep water followed a dimensionally consistent $ug f^{-4}$ form, Kitaigorodskii (1975) offered a revised basis for the equilibrium range in terms of nonlinear interactions. Nonlinear wave-wave interactions have been found to be capable of maintaining observed energy-flux balance in the equilibrium range (Resio et al., 2004). Within this equilibrium range principle, the appropriate power law is still not completely agreed upon.

The role of wave self-similarity will be considered to evaluate processes taking place in the nearshore environment in chapter 2, which presents an historical background on the theoretical approach of wave self-similarity throughout the last 50 years as a literature review. Following this general development of the similarity principles in chapter 2, this thesis analyzes data from the United States Army Corps of Engineer's Field Research Facility (FRF) in Duck, North Carolina obtained from the FRF 630 gauge situated at a 20-meter depth and the FRF 625 gauge stationed at an 8 meter depth. The wave spectra are categorized into three main groups: young sea, mature sea, and swell. Here the definition of young sea is related to the relative speed of waves at the spectral peak to the wind speed, with the term "small wave age" indicating that the waves are traveling much slower than the wind speed and larger wave ages indicating that the waves are propagating at speeds equal to or greater than the wind speed. For simplicity in these analyses, wave periods from 5 to 7 seconds are considered to be "young", mature seas will be taken as wave periods from 8 to 11 seconds, and swell will be taken as wave periods from 12

to 18 seconds. With the spectra being discussed, it is important to note that the focus is on clear situations that illustrate the physics of single wave trains (i.e. single-peaked spectra as opposed to multi-peaked spectra). More detail on this topic will follow in chapter three.

Chapter three provides a brief description of the data used and how they were categorized. Chapter four discusses methodologies used to relate these spectral forms to energy dissipation. Chapter five illustrates the results that were computed using the various methodologies discussed. Chapter six provides analyses of specific events within the data set that produce similarities and limitations to the equilibrium range in wave spectra. Ultimately, chapter seven concludes with an exposition of the investigation of this topic and recommendations for further research on wave self-similarity. Throughout time, many researchers have advanced different theoretical bases for nearshore energy dissipation. The spectral method in this thesis incorporates observed changes in spectral shape to provide a different perspective on this topic.

CHAPTER 2: HISTORICAL BACKGROUND

2.1 The Self-Similar Approach

Wave spectra has been the most reliable source of data for analyzing wave characteristics for the past few decades. Phillips (1958) introduced the equilibrium range in wave spectra for wind generated waves in deep water. This theory provided by Phillips demonstrated the spectrum in two different forms: wavenumber and frequency. Henceforth, the application of this concept in shallow water could be illustrated in wavenumber form. In the 1970's, scholars believed that bottom friction was the primary factor controlling the energy loss in nearshore wave environments. Therefore, another approach was developed to analyze other sources attributing to energy loss. Several tests were completed in the North Sea (Hasselmann et. al, 1973) to understand the source function that governs the fundamental energy balance. The Joint North Sea Wave Project (JONSWAP) showed the mechanism for swell attenuation was not clearly identified. In 1975, Kitaigorodskii applied the wavenumber spectrum on Phillips (1958) theory that illustrated similarity in finite depth water. Following into the next decade, Kitaigorodskii incorporated the f^{-5} scaling to show an equilibrium range within the spectral data used in 1983.

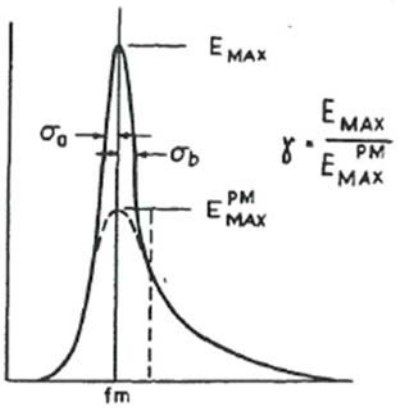

Figure 1. Definition of JONSWAP Coefficients (Hasselmann et al., 1973).

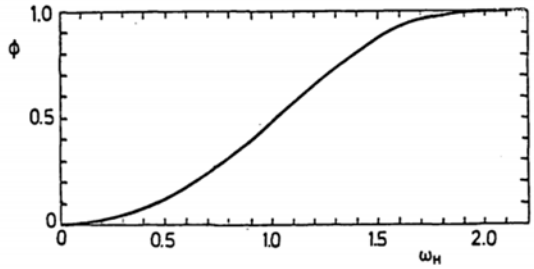

Figure 2. φ as a Function of ω_d (Kitagorodskii et al., 1975).

At this point, wave growth and decay in shallow water regions were not easily understood. The comparison of frequency and wavenumber space was compared in 1985 (Bouws et. al) for wind waves in a finite water depth with the application of similarity laws. This theory turned into the TMA spectrum. Bouws et. al. applied this to the JONSWAP spectrum. The basis of TMA spectrum exhibited the growth of waves could be analyzed by applying similarity principles instead of traditional techniques used in the past. The TMA conclusions show the self-similar shape is not strongly influenced by bottom conditions.

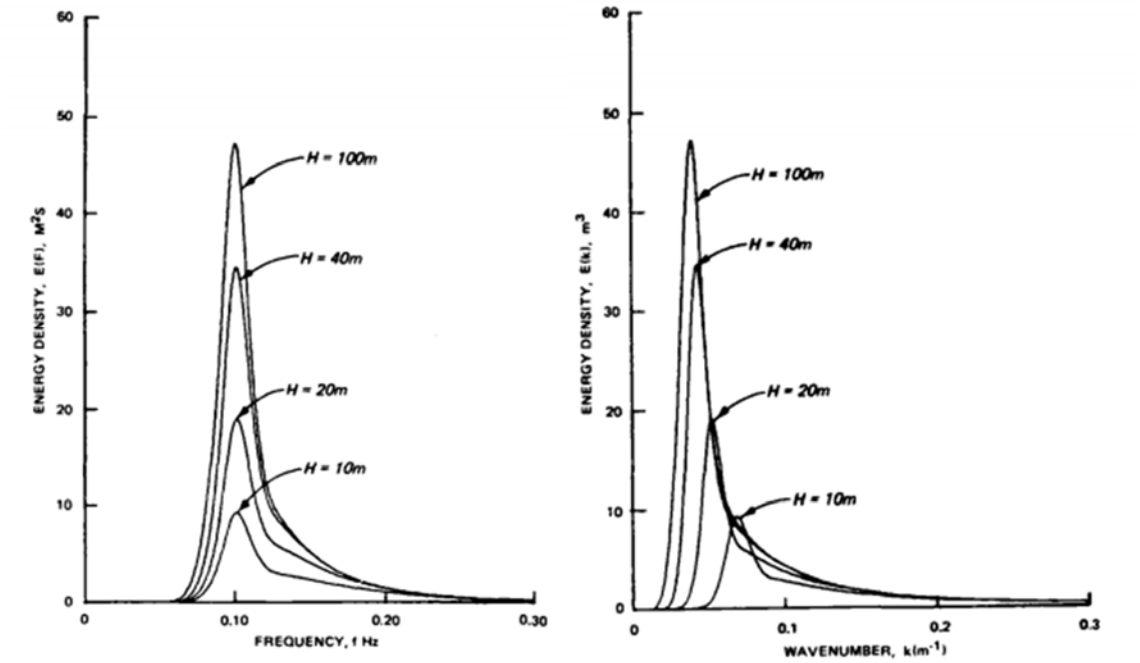

Figure 3. Wind wave spectra with JONSWAP parameters in TMA spectral form (Hughes, 1984) is shown on the right graphic compared to normal JONSWAP parameters on the left.

Resio and Perrie (1989) showed the f^{-4} equilibrium range was consistent with JONSWAP observations and could be incorporated and compared to the more frequently used f^{-5} scaling.

2.2 3rd Generation Wave Model and Parameterization Methods

At the turn of the century, Alves and Banner (2001) introduced a new formulation of the spectral dissipation source term. This parametrized source term is used in 3rd generation wave models today. The S_{ds} source term utilizes the behavior of deep water wave breaking associated with the nonlinear wave-wave interactions. Alves and Banner (2001) argued that this source term allowed greater flexibility in controlling the shape of the wave spectrum. Resio et al. (2004) proposed that nonlinear wave-wave interactions capable of maintaining the observed energy-flux balance in the equilibrium range. This established a firm theoretical basis for the equilibrium range and self-similarity in nearshore areas.

It is important to consider as much past research as possible in the assessment of nearshore wave energy dissipation. In the last 10 years, these parameterization methods have been the leading-edge solution in spectral wave modeling. Wave breaking is believed to be the dominant dissipative process contributing to S_{ds} source term (Alves and Banner, 2001). Physical wave parameterizations are typically accepted for operational applications if a model performs well in terms of significant wave heights, but the higher-order moments often have large errors (Stopa et al., 2016) and wave spectra are typically neglected in these comparisons. Moreover, existing parameterizations provide a reasonable distribution of breaking fronts for wave frequencies up to three times the dominant frequency but fail to replicate the observed reduction in breaking front lengths for shorter waves (Leckler et al., 2013). With that said, these parameterization methods work well in some areas, but fail to capture the evolution of the spectrum in wave propagating toward the coast. Therefore, another approach must be implemented to consider these shorter waves.

CHAPTER 3: DATA

The data used here were obtained from the U.S. Army Corps of Engineer's Research and Development Centers Field Research Facility (FRF, www.Frf.usace.army.mil), a site which is located on the east coast of the United States, situated at Duck, North Carolina as shown in Figure 4.

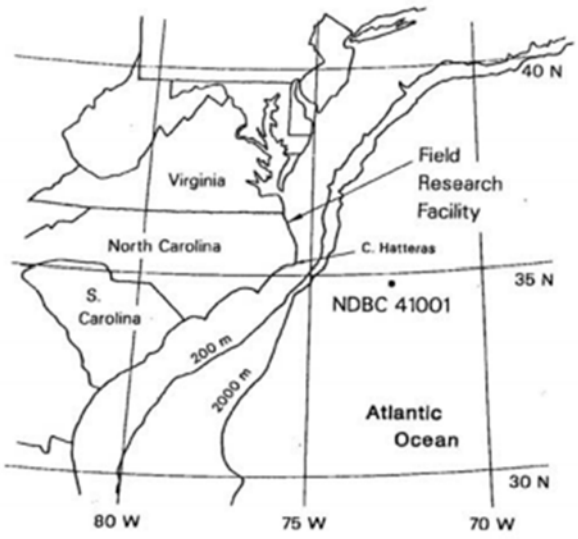

Figure 4. Field Research Facility located in Duck, North Carolina.

The two devices used for data collection include gauges from the FRF: the FRF gauge 630; a non-directional Waverider buoy located 6 km offshore (Figure 5); and the inshore buoy, FRF gauge 625; a Baylor gauge attached to the eastern end of the FRF pier located about 500 m offshore (Figure 5). The winds were measured from the seaward end of the FRF pier (Figure 6). An anemometer was used to estimate winds for FRF 625 and the FRF 630.The data collected by these two gauges were documented by energy density and frequencies. Both gauges documented the energy density per frequency for that specific Julian date (shown in Appendix A). The 630-gauge records 28 frequencies per Julian date and the 625-gauge records 18 frequencies in each observation.

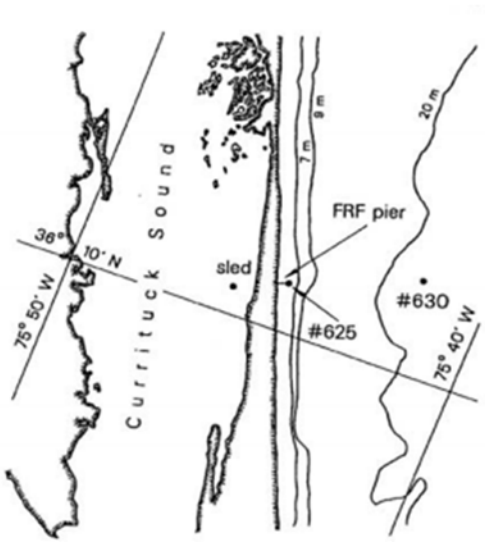

Figure 5. FRF gauge locations are shown. The FRF 630 gauge is at a depth of 20 meters and the FRF 625 gauge is at an 8 meter depth.

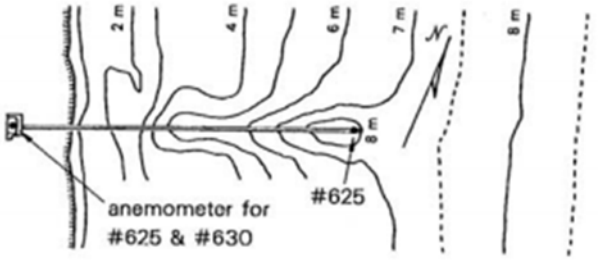

Figure 6. The anemometer used to estimate wind for FRF 625 and FRF 630.

Table 1. Wave spectra categories based off peak wave periods.

Category	Wave Period (seconds)
Young Sea	5-7
Mature Sea	8-11
Swell	12-18

The data sets were categorized into specific classes to analyze nearshore wave characteristics. Each category contains nearly 50 data sets from the FRF 625 gauge and the FRF 630 gauge. Thus, a wide range of wave spectra was examined for several equilibrium principles here. Table 1 shows the classification of the data into 3 groups: young sea, mature sea, and swell. These data were categorized based on their peak wave period. The categorization of these data sets is key to understanding how the equilibrium ranges are

affected by these power-law principles. The next chapter will discuss the methodological approach of the wave equilibrium range transformation from deep to shallow water.

CHAPTER 4: METHODOLOGY

In well-developed, wind-generated waves, Phillips (1958) proposed there should be a range of frequencies based on wave breaking. This occurs in frequencies that are higher than the spectral peak frequency which creates a range of equilibria. The equilibrium range form that Phillips suggested is

$$E_p(f) = \alpha g^2 f^{-5} (2\pi)^{-4} \qquad (1)$$

where f is frequency, g is gravity, and α is a constant. Wave spectra used by modern scientists still follow the PM (Pierson and Moskowitz 1964), JONSWAP, (Hasselmann et al., 1973), and The TMA (Texla Storm, MARSEN, and ARSLOE) spectrum (Bouws et al. 1985) theories, which are based on this f^{-5} form. The PM spectrum was adapted from Phillip's equilibrium range (1) and can be is shown as

$$E_{PM}(f) = E_p(f) e^{-5/4(\frac{f}{f_p})^{-4}} \qquad (2)$$

where f_p is the frequency at the spectral peak. The JONSWAP equation (Hasselmann et al., 1973) further modified the PM spectrum, by including a peak enhancement factor:

$$E_J(f) = E_p(f) e^{-\frac{5}{4\left(\frac{f}{fp}\right)}^{-4}} \gamma e^{[-(\frac{f}{f_{p-1}})^2/2\sigma^2]} \qquad (3)$$

where $E_p(f) = \alpha g^2 f^{-5} (2\pi)^{-4}$, $\sigma = .076(\frac{gX}{U})^{-0.22}$, X = fetch distance, U= wind speed, $\gamma = 7.0(\frac{gX}{U^2})^{-0.143}$, *and* f_p is the frequency at the spectral peak. The self-similar spectral form is used to a region of the spectrum that is called the equilibrium range. To make the x-axis non-dimensional, the frequency is divided by the peak frequency (given by the FRF gauge 630). This f/f_p is depicted in Figure 7:

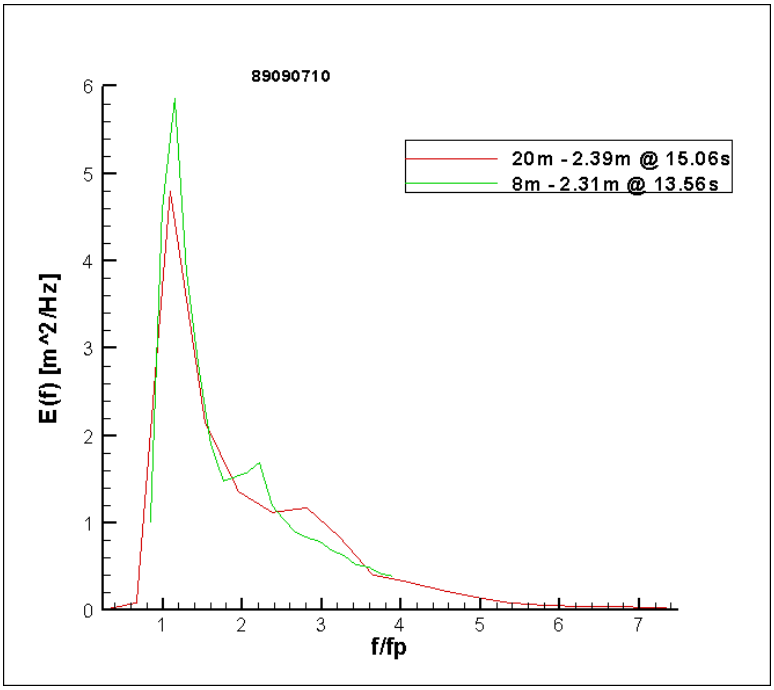

Figure 7. An example of the wave spectra data examined in energy density and f/f_p form.

As shown above, Bouws et al. (1985) showed that a conversion of the JONSWAP spectrum to a wavenumber form could be used to convert the JONSWAP spectrum to shallow water. This shallow-water transformation was confirmed by 2,000 selected wave spectra points known as the TMA spectrum. Equation 4 is the formulation based off the TMA spectrum:

$$E_{TMA} = E_K(f,H)\varphi_{PM}\left(\frac{f}{f_m}\right)\varphi_J(f, f_{m,}\gamma,\sigma) \qquad (4)$$

where $E_K(f,H) = \beta k^{-3}$.

The shallow water wave spectrum can be expressed in frequency form (*f* space) as provided, or the wavenumber form. Although almost all observations in wave spectra are illustrated in *f* space, the wave number domain (*k* space) is appropriate for investigating further into similarity laws especially in shallow water environments. Foremost, the wave number is related to the frequency by the dispersion relation

$$(2\pi f)^2 = gk\tanh(kh), \quad (5)$$

where h is water depth. Kitaigorodoskii et al. (1975) demonstrated the wave number spectrum sustains similarity in finite depth water. Translating the frequency domain to the wave number domain is developed by

$$k_i = f_i(\frac{1}{f_p}) \qquad (6)$$

where f_p is the peak frequency of the spectrum. Whereas, the equilibrium range develops is given by

$$F(k) = \beta k^{-3} \quad (7)$$

where β represents units of velocity and k is the wave number equal to 2π/L. Older studies show that the k^{-3} dependence is shown from deep water and into shallow water (Kitaigorodskii et. al, 1975 and Hughes, 1984 and Vincent, 1985). This k^{-3} scaling demonstrates a form of wave breaking due to wind input. Kitagorodskii et al. (1975) observed that both forms of the equilibrium range given for deep water, but could exist in shallow water as well based off Phillips (1958). Subsequently, waves experience wave breaking in both shallow and deep water; the similarity form could exist in depths in shallow water. Additionally, Hughes (1984) believed Equation 7 was thought to be a result of a limiting steepness at each frequency which wave breaking would occur in deep water. Moreover, any additional input in wave energy form would result in waves breaking and a transfer of wave energy from that frequency; these factors would be mechanisms of dissipation and wave-wave interactions. Most of the researchers throughout history (Kitaigorodskii et. al, 1975 and Hughes, 1984 and Vincent, 1985) describe the self-similarity principle that show the k^{-3} scaling dominates throughout deep to shallow water. Given this scaling, wave breaking is assumed dominant throughout the spectrum. Although k^{-3} has been used throughout deep to shallow water, this thesis also uses an approach that has been applied to analyze scalar wavenumber space and integrating the $k^{-5/2}$ scaling in deep water. Resio et al. (2004) presented that for finite depth wave spectra could be expressed in wave number-equivalent form as shown as equation (8)

$$F(k) = \beta g^{-1/2} k^{-5/2}, \qquad (8)$$

where *F(k)* is spectral energy density in wave number domain, *k* is the wave number, and β representing a coefficient with units of velocity.

A dimensionless parameter known as wave age will be investigated as a surrogate for wave steepness purposes. Wave age is the ratio of the phase speed of the spectral peak to the wind speed; typically, it is representative of the duration that the wind has been acting on a wave field. Therefore, the wind must be blowing for only a short time or the fetch is limited for waves to be considered "young". Mathematically, this parameter is given by

$$wave\ age = \frac{u}{c_p}\ , \qquad (9)$$

where u is the wind speed and c_p is the phase velocity at the spectral peak. For this thesis, wave age will be used to measure the stage of wave development during generation by the wind. Values near unity present full development for the measured windspeed, higher values suggest young, growing seas, and lower values suggest diminished wind forcing transitioning into swell.

CHAPTER 5: RESULTS

Although the equilibrium range has been studied for the past several decades, the specific source responsible for self-similarity in ocean waves remains uncertain. Still, the motive to introduce the ability of self-similarity and equilibrium range principles to improve our understanding of nearshore processes. Understanding this concept will benefit theories for wave energy dissipation in shallow water. In short, this approach will contribute to the improvement of shallow water wave models used today. The history of nearshore wave progression in a self-similar spectral form have shown k^{-3} dependence from deep to shallow water (Phillips, 1958, Kitagorodskii, 1975, Hughes, 1984 and Vincent, 1985). This thesis investigates the evolution of $k^{-5/2}$ to k^{-3} spectral shape from wave data at a 20-meter depth to an eight-meter depth.

5.1 k^{-3} Scaling for Wind-Generated Waves

Two important processes are examined in Figures 8-16: wave breaking and nonlinear interactions. Resio et al. (2004) examined wind waves subject to high wind speeds, fetches and peak spectral periods with equilibrium ranges well represented by $k^{-5/2}$. In correlation to that, the results illustrated from the FRF 630 and 625 gauges exhibit a similar form; the k^{-3} scaling proved to exist in shallow and deep water. Figure 8 shows the k^{-3} dependence in frequency space for waves in the young sea category (wave periods from 5 to 7 seconds).

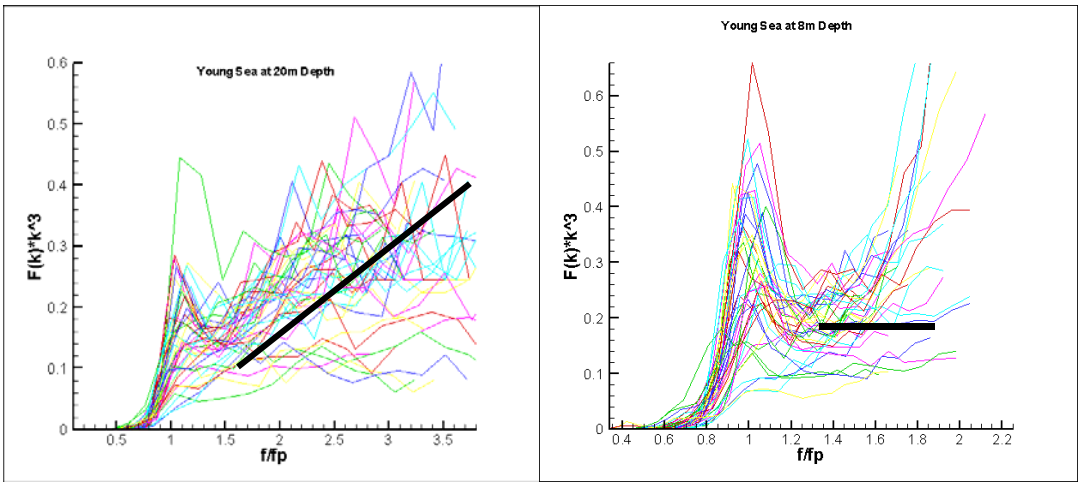

Figure 8. k^{-3} scaling for young sea at 20m to 8m depth demonstrates an upward slanting line indicating waves in deep water are gaining energy. In shallow water, the horizontal line indicates the wave energies staying constant (equilibrium).

As shown in Figure 8, a shift to the k^{-3} scaling tends to become more pronounced at the shallower gauge for these cases. At the deeper gauge, the wave energy in young sea waves show a wide range of stability within the spectrum. In deeper water, the young seas do not reflect wave breaking based off the mean direction of the spectrum since energy is not being lost. In contrast, the data at the gauge nearshore portray an equilibrium range that satisfies the self-similarity concept k^{-3} scaling based off the equilibrium shape most of the spectra it reaches. Therefore, the young sea in shallow water exhibits nonlinear wave-wave interactions as it stays almost constant throughout a section of the spectra. As shown above in shallow water, the young sea with k^{-3} dependence appears to be generating a second harmonic. This second harmonic shows nonlinearities within the young sea waves approaching the coastline. Figure 9 shows the k^{-3} dependence in frequency space for waves in the mature sea category (wave periods from 8 to 11 seconds).

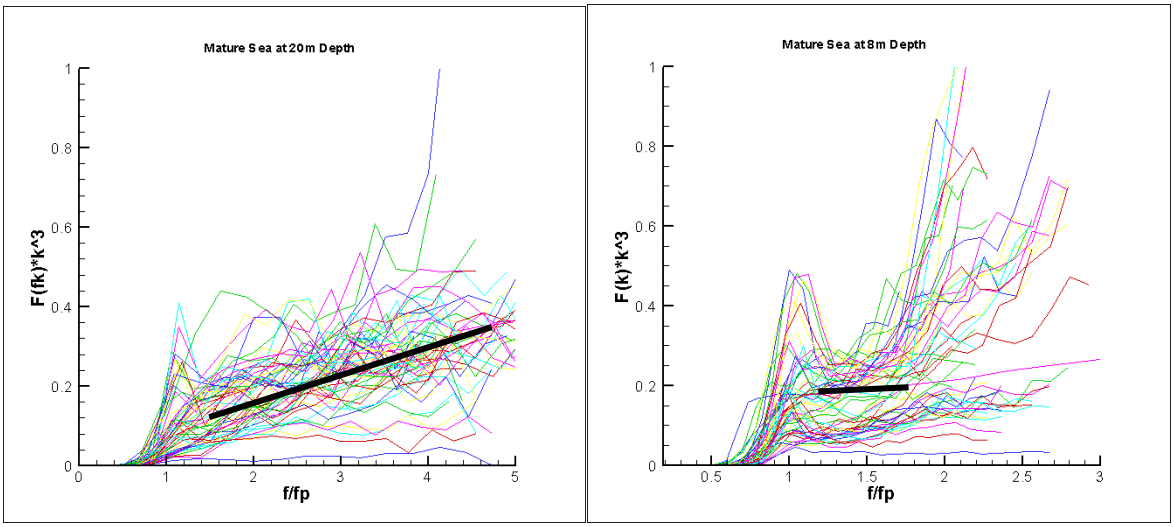

Figure 9. k^{-3} scaling for mature sea at 20m to 8m depth demonstrates an upward slanting line indicating waves in deep water are gaining energy. In shallow water, the horizontal line suggests the lower energy waves staying constant with instabilities across the spectrum.

The k^{-3} scaling in wave spectra data categorized at mature sea waves provides a similar illustration to the results above for young sea waves. The mature sea in deeper water portray a better fit to the k^{-3} scaling until the dimensionalized *f/fp* reaches two on the x-axis. After two, the spectra start gaining more energy. This does not resemble a spectrum dominated only by wave breaking. As shown in Figure 9, a similarity pattern is portrayed more clearly in the FRF 625 gauge at an eight-meter depth. Thus, wave spectra with peak periods under 12 seconds exemplify the k^{-3} scaling as recent scholars have shown (Kitaigorodskii et. al, 1975, Hughes, 1984 and Vincent, 1985). The mature sea in shallow water exemplify more of a k^{-3} dependence, similar to the young sea in shallow water. This shows that mature sea waves in shallow water are dominated more by wave breaking than in deeper water with partial nonlinear wave-wave interactions taking place; however, the dominant source is still to be determined. Figure 10 shows the k^{-3} dependence in frequency space for waves in the swell category (wave periods from 12 to 18 seconds).

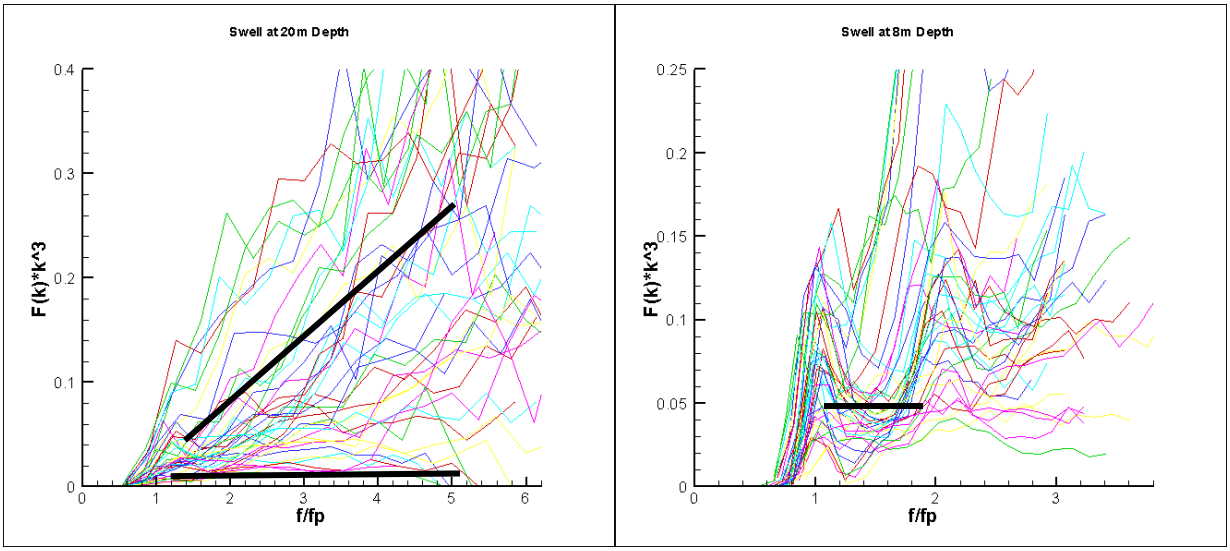

Figure 10. k^{-3} scaling for swell at 20m to 8m depth demonstrates an upward slanting line indicating waves in deep water are gaining energy with lower energy waves behaving with constant energy. In shallow water, the horizontal line shows the waves reaching 2nd and 3rd harmonics.

As shown in Figure 10, the k^{-3} scaling suggests a transition in form from the deep to the shallow depths in the equilibrium range within the wave spectrum. At the deeper gauge, the wave energy in swell waves show a scattered distribution of wave energy throughout the spectrum. Moreover, the data at the gauge nearshore portrays an equilibrium range that follows the self-similarity pattern with a second harmonic as it translates through frequency space within the spectrum. For some of the waves with more energy, more than two harmonics are present within the spectrum. The self-similarity for swell displays a wide range of variability; therefore, the swell spectrum should be noted with superposed harmonic. The swell waves with less energy still portray a small k^{-3} dependence, but for most of the spectra, the swell waves in deeper water are portraying more harmonics that illustrate very nonlinear waves. Based off the analysis, the compensated spectra do not resemble wave breaking in deep water. In shallow water, the equilibrium is shown with harmonics across the spectra. The data set for swell in shallow water display k^{-3} dependence (wave breaking) with harmonics. This means that swell spectra are dominated by wave breaking, but still have limitations due to the nonlinearities.

These results were intended to recreate the self-similarity and equilibrium theories proposed by researchers throughout history (Kitagorodskii, 1983, Hughes, 1984 and Vincent, 1985). On the contrary, the other self-similarity form proposed by Resio et al. (2004) presents a scaling that incorporates a $k^{-5/2}$ dependence in scalar wave frequency space.

5.2 $k^{-5/2}$ Scaling for Wind-Generated Waves

The proposed method in this thesis is an adjustment to the equilibrium range that integrates the theories presented in the past with a slight modification in the scaling for a different approach to investigate self-similarity. Figure 11 incorporates the $k^{-5/2}$ scaling from deep to shallow water in young seas (periods 5 to 7 seconds).

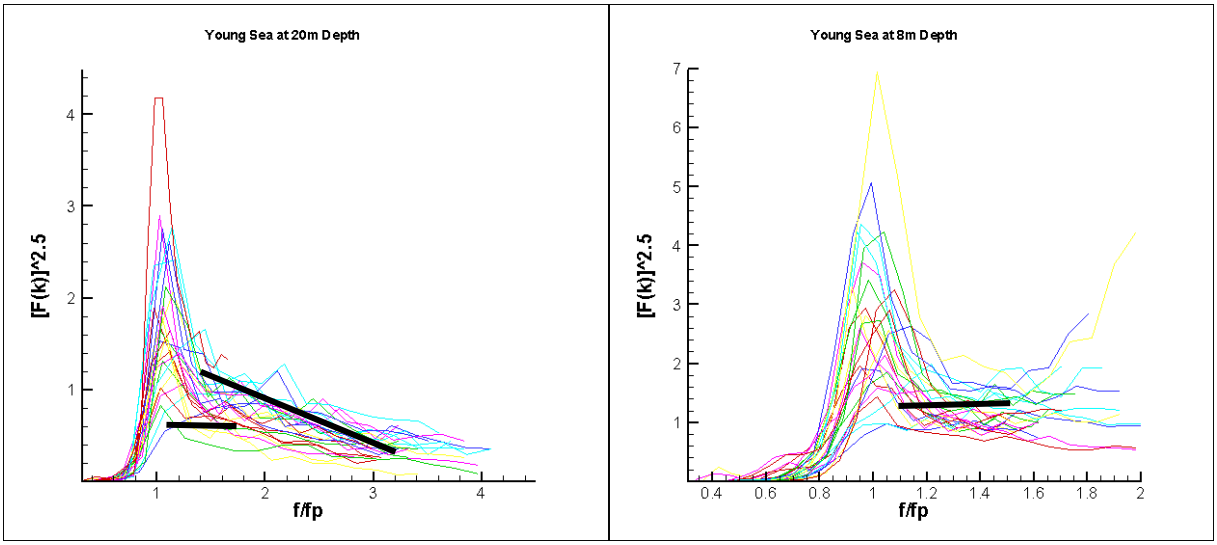

Figure 11. $k^{-5/2}$ scaling for young sea at 20m to 8m depth exemplify a constant decrease in energy in deep water. In shallow water, the horizontal line indicates constant energy across the spectrum.

The $k^{-5/2}$ scaling in wave spectra data categorized at young sea waves provides a self-similar response in the frequency domain. Figure 11 demonstrates the $k^{-5/2}$ scaling in deep water within the young sea

data set. This approach maintains the same self-similarity principles in shallow water. The fit for the $k^{-5/2}$ dependence in shallow water suggests that there is another source that is controlling the equilibrium range in the energy spectra in deep water. For young sea waves in deep water, the $k^{-5/2}$ scaling controls the spectrum until the waves start losing energy because of wave breaking. This suggests that the spectrum has a mix of both nonlinearity and wave breaking at the end of the spectrum in deeper water. On the contrary, the spectrum for young sea in shallow water portray an equilibrium range across the spectrum more consistently than those in deeper water. Much wave breaking does exist at an eight-meter depth, but the young sea in shallow water is dominated by wave-wave interactions. The interactions in young sea are stronger in shallow water; therefore, more of the spectrum is dominated due to the constant energy across the spectrum. Figure 12 illustrates the equilibrium range in the $k^{-5/2}$ for the mature sea data set. As shown in Figure 11 (young sea), the FRF 630 gauge provides an equilibrium range that is more consistent within the wave spectrum. Like the young sea data set, the mature sea wave characteristics in deep water follow $k^{-5/2}$ scaling. Figure 13 incorporates the $k^{-5/2}$ scaling from mature seas (periods 8 to 11 seconds).

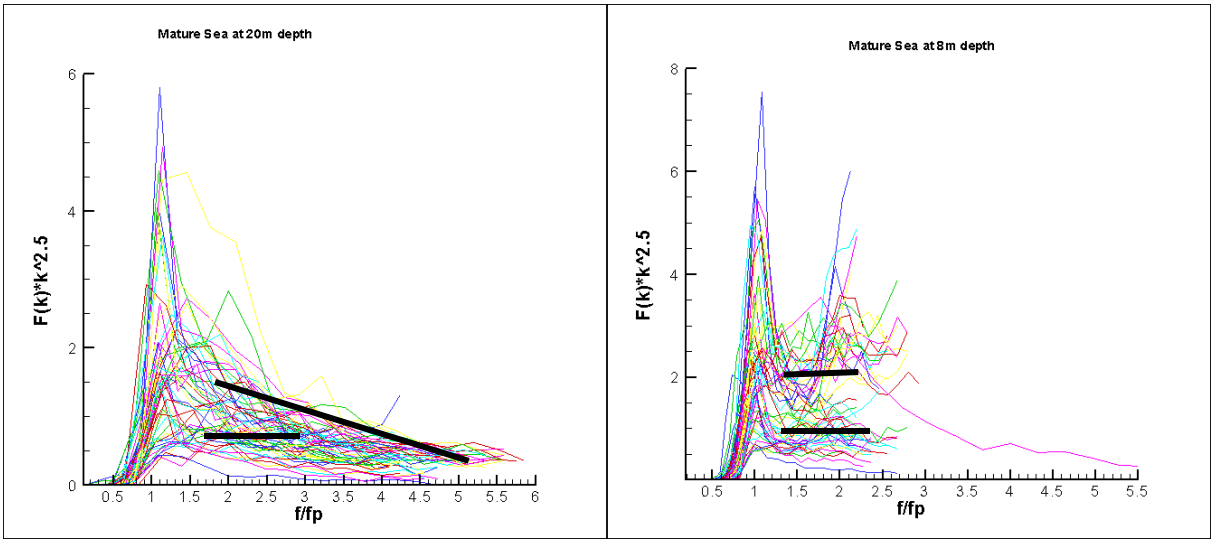

Figure 12. $k^{-5/2}$ scaling for mature sea at 20m to 8m depth portray a constant decrease in energy in deep water. The shallow water spectrum is self-similar within the higher energy waves and lower energy waves.

The $k^{-5/2}$ scaling in wave spectra data categorized at mature sea waves provides a similar illustration to the results above for young sea waves Figure 11. Although the $k^{-5/2}$ dependence in shallow water portrays some equilibrium, it does not fit as well compared to the k^{-3} in shallow water (Figure 9). As shown in Figure 12, the 20-meter gauge provides an equilibrium range that is more consistent within the wave spectrum. For deep water, the similarity principles show the $k^{-5/2}$ scaling dominants the spectrum. This shows an equilibrium range does exist within the spectra with lower energy waves. The higher energy waves do resemble nonlinear wave-wave interactions, but wave breaking still does exist due to their decrease in energy at a faster rate. In shallow water, the spectrum is dominated by wave-wave interactions. The waves with more energy reach a second harmonic, which illustrates more nonlinearities. For the most part, the $k^{-5/2}$ dependence for mature sea waves in shallow water provide an equilibrium range that shows nonlinear wave-wave interactions throughout the entire spectrum with a slight decrease in energy for the lower energy waves as they start breaking. Figure 13 shows swell with $k^{-5/2}$ scaling:

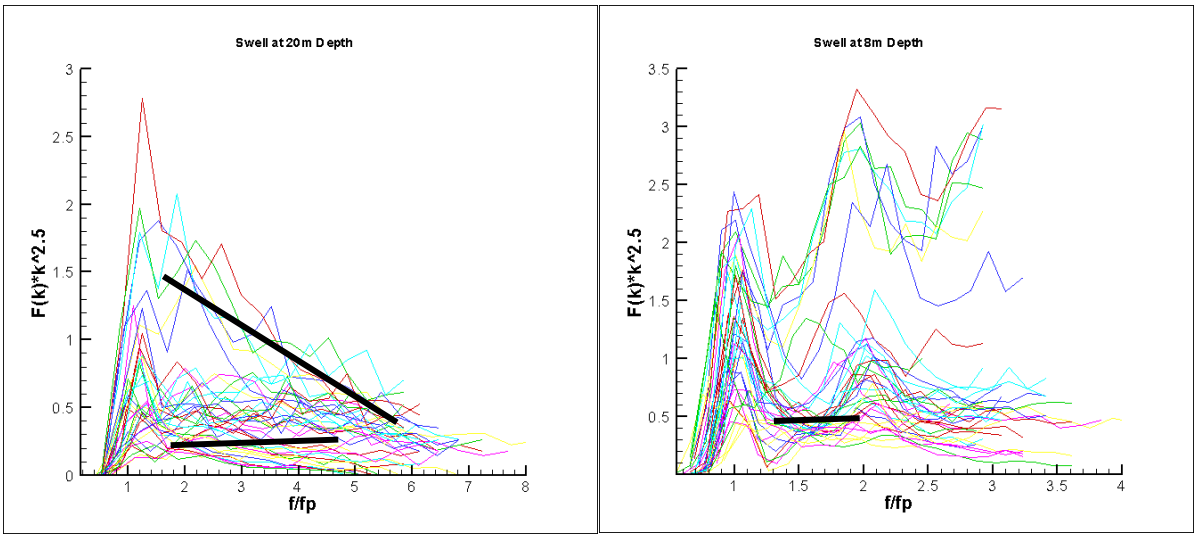

Figure 13. $k^{-5/2}$ scaling for swell at 20m to 8m depth illustrate higher energy waves breaking in deep water with lower energy waves staying constant across the spectrum. In shallow water, the swell waves approach 2nd and 3rd harmonics.

The $k^{-5/2}$ scaling in wave spectra data categorized at swell waves does not have a similar shape compared to the young and mature sea waves. In deeper water, the larger waves are decreasing in energy

across the spectrum at a faster rate which portrays wave breaking. The lower energy waves in deep water show an equilibrium range that slightly decreases across the spectrum. This shows wave breaking and nonlinear wave-wave interactions do exist. In shallow water, the swell waves illustrate a 2nd harmonic in the nearshore regions as shown in Figure 13 which is like k^{-3} scaling for swell. The swell spectra in shallow water are very nonlinear. This shows that the similarity principles have limitations for waves with high peak periods (swell) for both the $k^{-5/2}$ and k^{-3} power laws.

5.3 k^{-3} Scaling for Wind-Generated Waves

Since both scaling's have been introduced, the idea presented in the following figures will show how each scaling transforms from deep water to shallow water. With that said, this approach will set up the $k^{-5/2}$ scaling in deep water and incorporate the k^{-3} scaling in shallow water. The deep water self-similarity theory expressed by Phillips (1958) in wavenumber or frequency form was investigated by Kitaigorodskii et al. (1975) to show the same k^{-3} relation for deep and shallow water. On the other hand, Resio et al. (2004) provided an equilibrium range in wind-generated wave spectra that is characterized by a $k^{-5/2}$ form. This thesis proposes a relation of the $k^{-5/2}$ dependence in deep water and k^{-3} dependence in the shallow water regions. Furthermore, this new concept combines past researcher's hypotheses (Kitagorodskii et al. 1975 and Resio et al. 2004) to provide another approach to estimate nearshore wave attenuation.

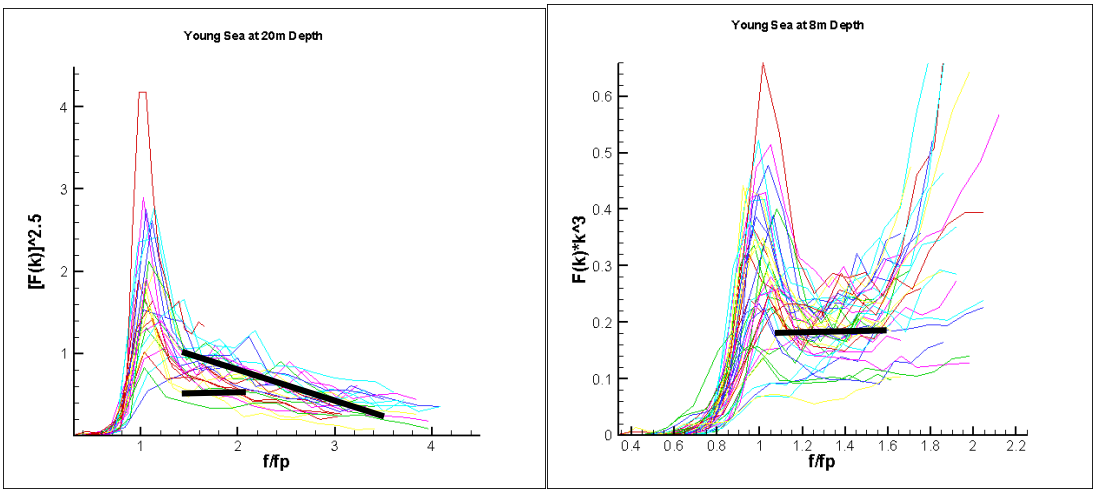

Figure 14. $k^{-5/2}$ to k^{-3} scaling for young sea at 20m to 8m depth exemplify a gradual decrease in energy in deep water. Constant energy across the spectrum is shown in shallow water.

Figure 14 portrays the young sea wave spectra in frequency form translating from $k^{-5/2}$ to k^{-3}. This transformation from deep to shallow water in waves with periods under eight seconds provides an equilibrium range that satisfies the self-similarity spectrum. As discussed previously, the young sea waves are dominated by nonlinear wave-wave interactions based on their equilibrium in shallow water. As the waves approach the shore, they are gaining energy due to interactions before they break. Proposing this transformation of scaling in waves with peak periods under eight seconds shows another way to look at the spectrum.

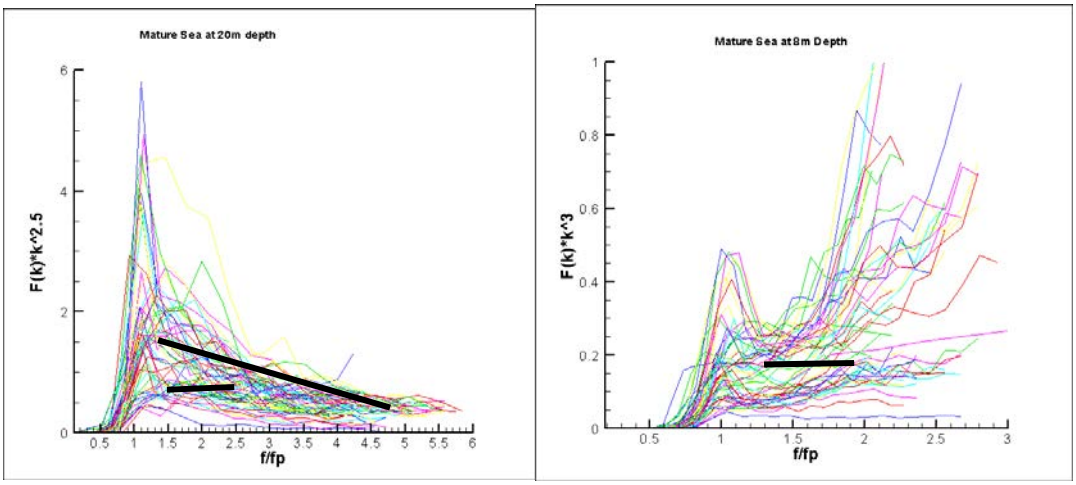

Figure 15. $k^{-5/2}$ to k^{-3} scaling for mature sea at 20m to 8m depth show a downward sloping line indicating a loss of energy within the spectrum in deep water for higher energy waves with lower energy

waves staying constant with a gradual loss of energy. The higher energy waves in shallow water do not exemplify a constant equilibrium range across the spectrum.

Figure 15 shows $k^{-5/2}$ to k^{-3} scaling for data categorized as mature sea waves provides a similar illustration to the results above for young sea waves. The mature sea waves do not resemble wave-wave interactions as dominant as young sea waves. As shown in Figure 15, the FRF 630 gauge provides an equilibrium range more consistent within the wave spectrum in deep water than k^{-3} (Figure 9). The k^{-3} in deep water provides a wider range of stability within the spectrum. The $k^{-5/2}$ scaling shows more of an equilibrium range that provides a cohesion of wave-wave interactions and wave breaking. Therefore, analyzing mature sea waves is very complex. Two processes (wave breaking and nonlinear wave-wave interactions) are taking place within certain regions of the spectrum in deep water. With that said, the higher energy waves have more wave breaking while still maintaining a minimal constant energy throughout the spectrum. On the contrary, the lower energy waves maintain constant energy for a larger portion of the spectrum. The shallow water spectra for mature sea waves all provide constant energy across the spectrum. Therefore, nonlinear wave-wave interactions are more dominant within the lower energy waves within the spectra for mature sea waves. Figure 16 shows the transformation of scales for swell:

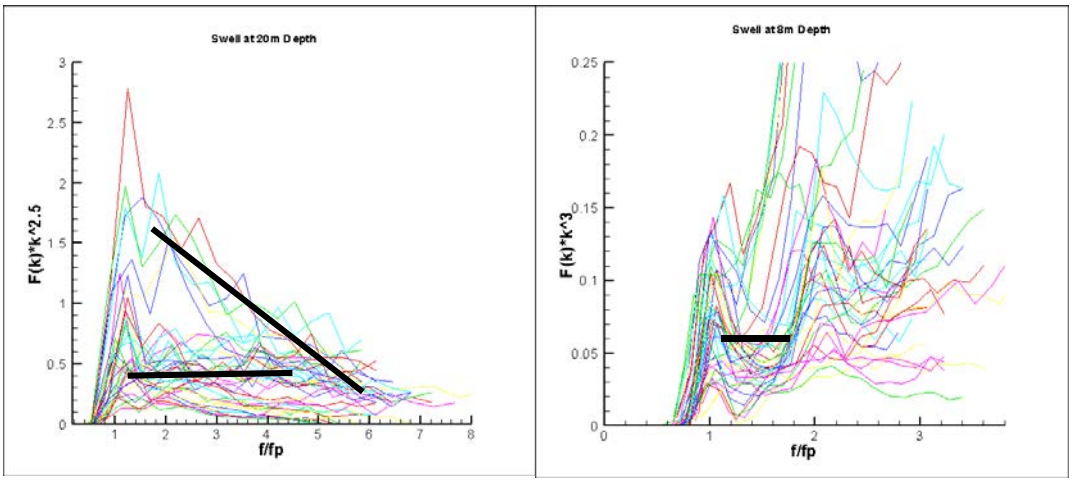

Figure 16: $k^{-5/2}$ to k^{-3} scaling for swell at 20m to 8m depth. The downward sloping line indicates a rapid loss of energy within the spectrum in deep water for higher energy waves with lower energy waves staying constant. The shallow water swell waves reach 2nd and 3rd harmonics.

Although the self-similarity principle has limitations to the category of swell waves, the $k^{-5/2}$ in deep water seems to have a better fit than Figure 10**.** Swell with a k^{-3} scaling does not portray stability within the spectrum as compared to the $k^{-5/2}$ in deep water. This scaling in deep water shows the larger waves dominated by breaking, due to their large amount of energy being lost. The smaller energy waves seem to have both wave breaking and nonlinear wave-wave interactions characteristics. Additionally, a 2nd and 3rd harmonic is shown for swell in shallow water with a k^{-3} form. As stated previously these harmonics are due to how nonlinear these longer period waves become as they approach the coastline.

5.4 Stage of Wave Development by Wind Generation

To examine the data set in more detail, wave age is analyzed to show the measure of the stage of wave development during generation by the wind. Figures 17-19 illustrate the parameter u/c_p , Equation 8, relative to the ratio of the wave height from deep to shallow water. Figure 17 shows the ratio of wave height from deep to shallow water relative to the wave age. Wind input is a primary factor within these waves. The region over one shows there is energy gained due to wind input. Also, it is shown below that there is a region of energy loss due to wave breaking. These wave ages are less than 1. Figure 18 shows mature sea wave obtain values between 0.8 and 1. This region is considered an intermediate zone. The mature sea waves are not quite old enough to become swell waves, but have wave periods higher than eight seconds. The source of energy loss is not clear. The cause of this is partially due to wave breaking, but the primary source needs to be investigated further.

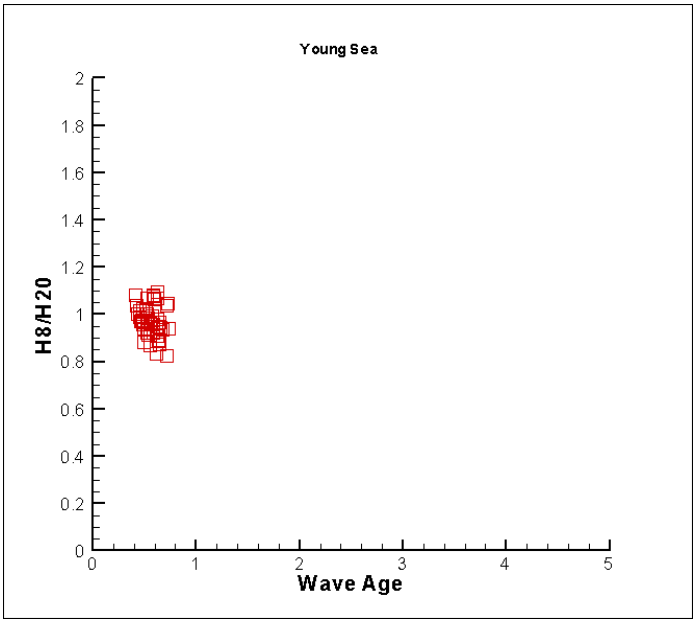

Figure 17. Wave age for young sea indicate values of wave ages less than 1. Wind input dominates the young sea data set.

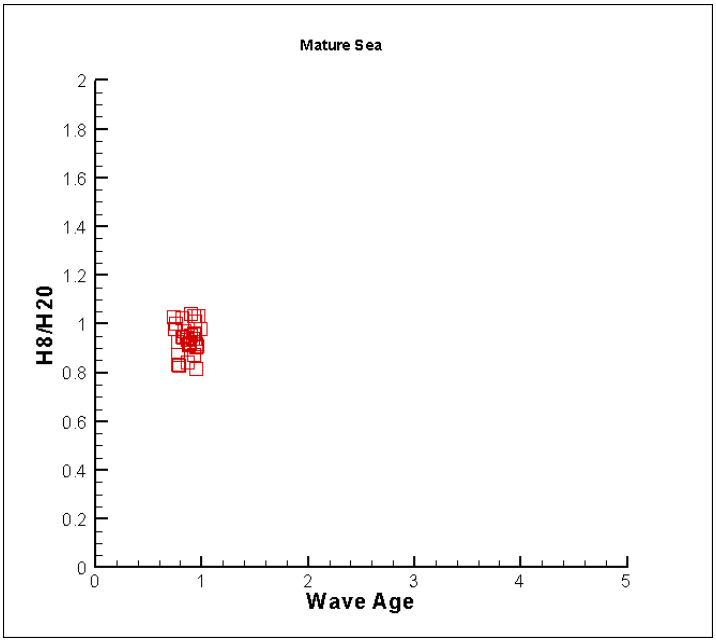

Figure 18. Wave age for mature sea indicate values of wave ages between 0.8 – 1. This is known as an intermediate range.

oun 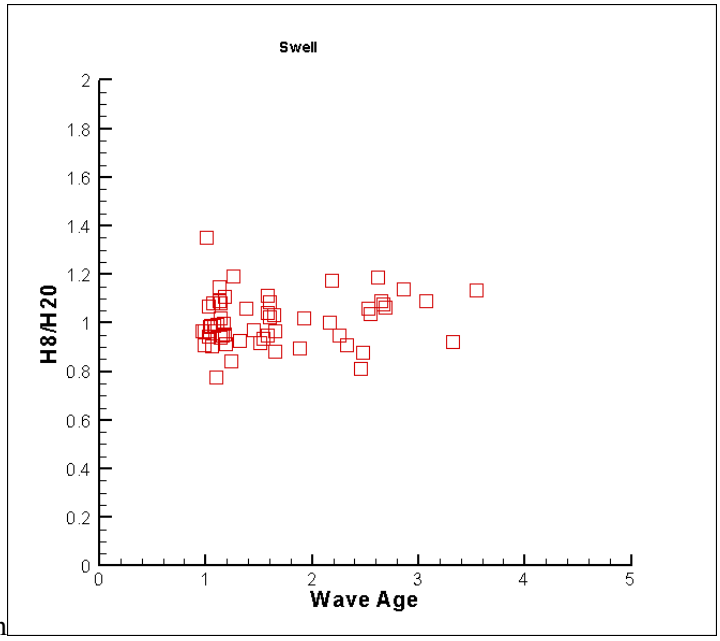

Figure 19. Wave age for swell indicate values of wave ages over 1. The wave ages for swell portray a gain in energy due to longer wave periods.

The swell spectra predominantly show a gain in energy. As shown in Figure 19, there are cases from 1 to about 4, with an outlier. These larger quantities could be due to shoaling since these waves have very long wave periods. Some of the samples become smaller. These samples have shorter wave periods which begin to break. For the present data, $0.4 < u_{10}/c_p < 6$, indicating these observations extend from the swell domain through full development to include some very young seas. This range incorporates most conditions of practical wave characteristic scenarios in nature, but does not encompass into conditions of research laboratory wind flumes. The concept of $k^{-5/2}$ dependence in deep water transforming into k^{-3} dependence in shallow water has been introduced in this thesis. The next section will discuss several cases within each category.

CHAPTER 6: DISCUSSION

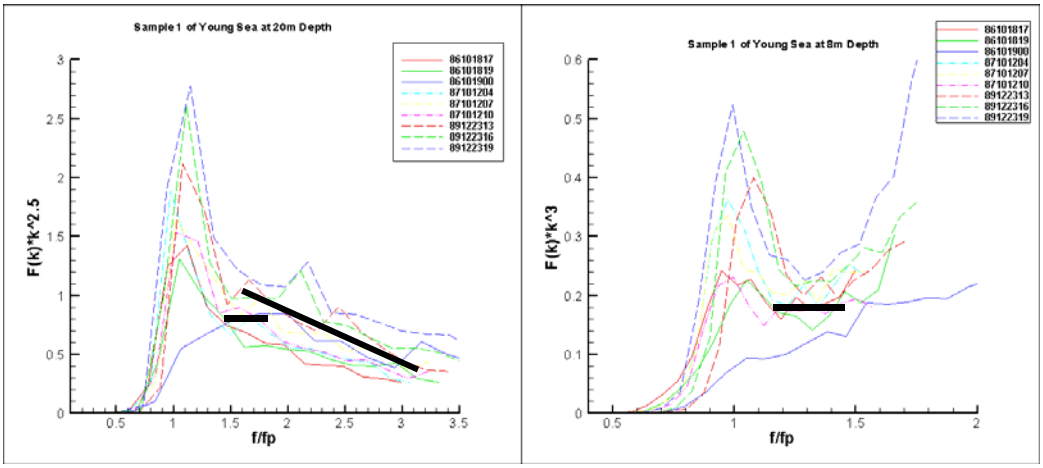

Figure 20. Young sea data comparison illustrates exemplify a constant decrease in energy in deep water. In shallow water, a constant energy across the spectrum is demonstrated.

As shown in Appendix A, the three data sets for young sea represent specific cases that occurred in 1986, 1987, 1989. These wave spectra were selected due for a comparison of wave data sets that fell under the criteria of being over 2 meters in significant wave height, and peak wave periods recorded under 8 seconds. Although these data sets were recorded over a year apart from each other, the wave characteristics portray a consistent equilibrium behavior in deep water that shows both nonlinear wave-wave interactions and wave breaking as the waves reach higher frequencies along the spectrum. In shallow water, the young sea waves show an equilibrium range dominating as a constant energy is displayed across the spectrum. This illustrates wave-wave interactions in shallow water. The nonlinearities show energy being gained as it approaches shallower water.

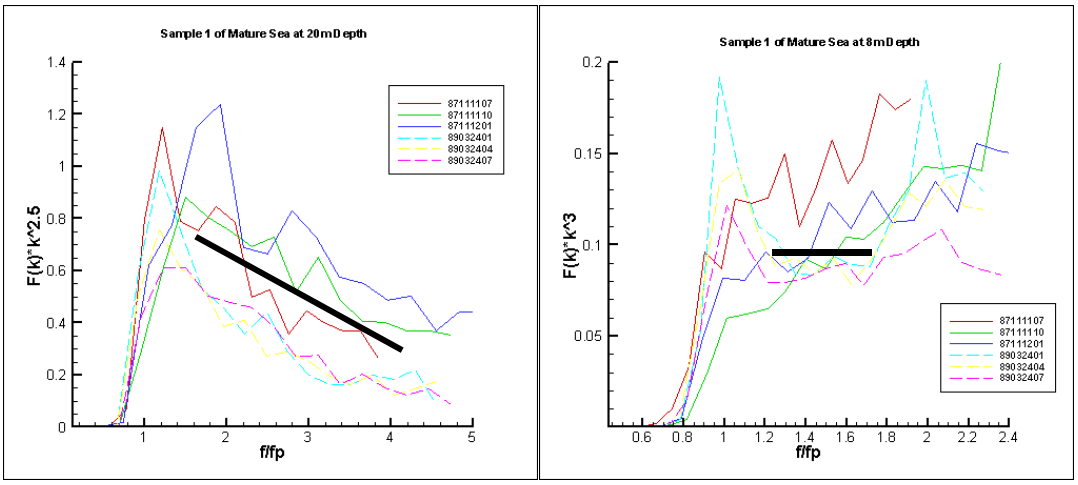

Figure 21. Sample 1 of mature sea comparison show breaking dominant in deep water. Smaller mature sea waves portray very minimal self-similarity in shallow water.

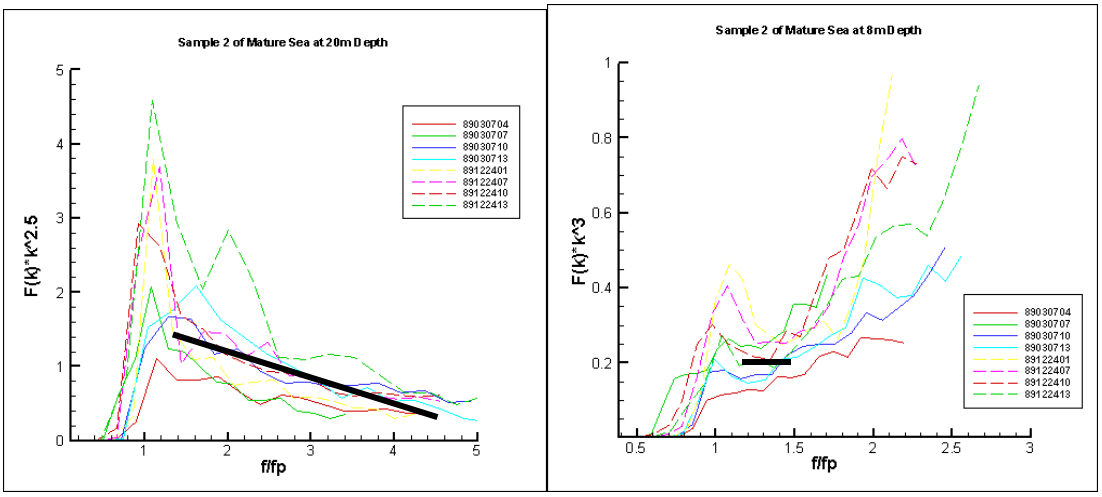

Figure 22. Sample 2 of mature sea comparison demonstrate wave breaking is dominant in deep water. Larger mature sea waves are dominated by 2nd harmonics in shallow water.

Moving forward, the next comparison is the mature sea spectrum. The first sample of mature sea data comparison considers wave characteristics that include significant wave heights between 2 and 3 meters with peak wave periods between 8 and 12 seconds. Sample 2 reflects wave characteristics that comprise of significant wave heights that exceed 3 meters and peak wave periods that stay in a consistent with the first sample of mature sea data. Hence, in deep water, Appendix A shows a stronger wind input which maintains a more dominant self-similar form. Therefore, mature sea waves with more energy exemplify

wave breaking mixed in with nonlinear wave-wave interactions. In shallow water both samples obtain second harmonics. The dominant source within the mature sea is a mix of both wave breaking and nonlinear wave-wave interactions. Thus, the mature sea wave source of dissipation is more complex.

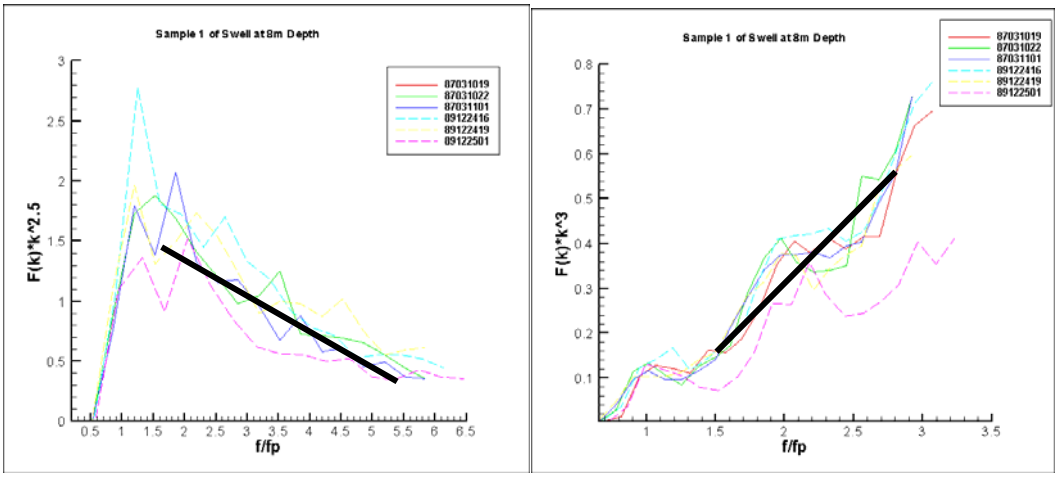

Figure 23. Sample 1 of swell comparison exemplify wave breaking is dominant in deep water. Larger swell in shallow water is dominated by 2nd and 3rd harmonics.

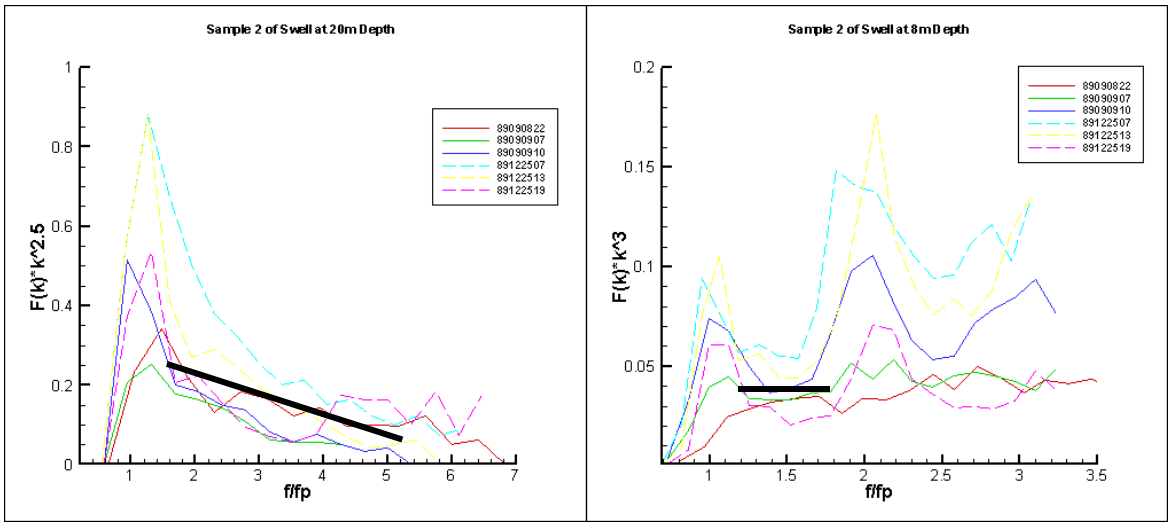

Figure 24. Sample 2 of swell comparison portray wave breaking is dominant in deep water. The smaller swell comparison show more similarity in shallow water compared to sample 2.

Figures 23 and 24 exemplify the cases for swell translating from the deep water to the coast with peak wave periods above 12 seconds. The first sample represents waves that exceed over four feet in significant wave height. As shown in figure 23, the two data sets from sample 1 epitomize large swell

coming from the offshore from storms. On the contrary, wave information for sample 2 encompass significant wave heights under three meters. The wave spectra from with $k^{-5/2}$ scaling in deep water satisfies the equilibrium range theory samples 1 and 2. Hence, the spectra in both samples show constant energy loss with wave breaking dominated in the larger energy waves. When the wave spectra enters shallow water and becomes k^{-3} dependence, the wave self-similarity principle have limitations within the swell data sets. Several harmonics are shown after the wave loses its initial energy. These harmonics are likely due to the nonlinearities within the waves approaching the coastline. This is a result of the waves representing longer-period swell, which have much narrow spreading in both direction and frequency. Based off the investigation of this thesis, the larger the significant wave height, the more increasingly dominant the harmonics become in shallow water with k^{-3} dependence. Therefore, the wave spectra equilibrium range in waves with peak periods above 12 seconds are not portrayed as well compared to waves with smaller peak periods; these larger period waves have limitations within the wave self-similarity concepts.

CHAPTER 7: CONCLUSIONS

An examination of data sets from the FRF at Duck, North Carolina that contained the FRF 630-gauge at 20-meter depth and the FRF 625-gauge at an eight-meter depth illustrated the attenuation of waves as they approach the coastline. The evolution of high wind wave spectra in shallow water exhibits a self-similar relationship with deviations suggestive of harmonics relative to the spectral peak. Furthermore, this data analysis has shown the following: (1) wind waves subject to a large range of wind speeds, fetches and peak spectral periods have equilibrium ranges reasonably represented by a $k^{-5/2}$ spectral form at the FRF 630 gauge at the 20-meter depth and k^{-3} spectral form at the FRF 625 gauge in 8-meters depth for young sea, with mature sea waves and swell having limitations; (2) energy levels within the equilibrium range can be characterized by a universal relationship involving wind speed and phase speed of the spectral peak, even for locations in moderately shallow water. Young sea waves are dominated by nonlinear wave-wave interactions in the nearshore. Similar to the influence of the TMA spectrum, nearshore wave models need to incorporate the self-similarity concept in deep and shallow water.

With that said, very interesting patterns have been portrayed based on the results of this thesis; these patterns can be refined. In the future, more wave spectra should be looked at with different cases that provide a larger window of wave directions. Analyzing larger swell cases in different regions of the world would benefit the research on this concept. Also, incorporating bottom friction within the self-similarity principles would provide a more accurate representation of the sources controlling the spectrum. An energy balance that can be moved into the numerical modeling range would be ideal for pushing forward with nearshore wave modeling.

REFERENCES

Alves, J. H. G. M., and M.L. Banner (2001). Performance of a saturation-based dissipation-rate source term, I, Modeling the fetch-limited evolution of wind waves, *J. Phys. Oceanogr*., 33, 1274-1298.

Bouws, E., Gunther, H., Rosenthal, W., Vincent, C.L., (1985). Similarity of the wind wave spectrum in finite depth water, Part I – Spectral Form, *J. Geophys. Res*., 90(C1), 975-986.

Hasselmann, K., Barnett, T. P., Bouws, E., Carlson, H., Cartwright, D.E., Enke, K., Eqing, J.A., Gienapp, H., (1973). Measurements of wind-wave growth and swell decay during JONSWAP, Ergänzungsheft Dtsch. Hydrogr. Z., 12, 95 pp.

Hughes S. A. (1984). The TMA Shallow-Water Spectrum Description and Applications, *Tech. Report CERC*-84-7. Coastal Engineering Research Center, Vicksburg, MS.

Kitaigorodskii, S. A., Krasitskii, V.P., Zaslavskii, M.M., (1975). On Phillips' theory of the equilibrium range in the spectrum of wind-generated gravity waves, *J. Phys. Oceanogr*., 5, 410-420.

Kitaigorodskii, S. A. (1983). On the theory of the equilibrium range in the spectrum of wind-generated gravity waves, *J. Phys. Oceanogr*., 13, 816-826.

Leckler, F.; Ardhuin, F.; Filipot, J.F. and A. Mironov, (2013). Dissipation source terms and whitecap statistics *Ocean Model*., 2013, 70 (9), 62-74.

Philips, O. M. (1958). The equilibrium range in the spectrum of wind-generated waves, *J. Fluid Mech*., 4, 426-434.

Pierson, W. J., and L. Moskowitz (1964). A proposed spectral form for fully developed wind seas based on the similarity theory of S. A. Kitaigorodskii. *Journal of Geophys Res.*, 69, 5181–5190.

Resio, D.T., and W. Perrie (1988). Implications of an f^{-4} equilibrium range for wind-generated waves, *J. Phys. Oceanogr*., 19, 193-204.

Resio, D.T., C.E., Long, and C.L. Vincent (2004). Equilibrium-range constant in wind-generated wave spectra, *J. Geophys. Res*., 109, C01018.

Stopa, J., Fabrice, A., Alexander, B., Stefan, Z., (2016). Comparison and validations of physical wave parameterizations in spectral wave models, *Ocean Modeling*, 103, 2-17.

Vincent, C.L., (1985). Depth Controlled Wave Height, *Journal of the Waterway, Port, Coastal and Ocean Division,* ASCE, Vol. 111, No.3.

Appendix A

Young Sea Sample 1 at 8m and 20m Depth

IDT	JZ	NF	HMO	TP	THp	Dep	wkph	WS	WD
86101817	7001	28	2.12	6.59	28.0			12.20	18.90
86101817	7001	18	2.23	6.24					

IDT	JZ	NF	HMO	TP	THp	Dep	wkph	WS	WD
86101819	7003	28	2.17	7.04	16.0			12.70	27.80
86101819	7003	18	2.21	6.92					

IDT	JZ	NF	HMO	TP	THp	Dep	wkph	WS	WD
86101900	7008	28	2.05	8.16	-6.00			12.70	22.30
86101900	7008	18	2.21	8.53					

IDT	JZ	NF	HMO	TP	THp	Dep	wkph	WS	WD
87101204	15604	28	2.33	7.04	2.00			14.70	16.00
87101204	15604	18	2.39	6.40					

IDT	JZ	NF	HMO	TP	THp	Dep	wkph	WS	WD
87101207	15607	28	2.32	7.04	-2.00			15.10	8.30
87101207	15607	18	2.42	6.74					

IDT	JZ	NF	HMO	TP	THp	Dep	wkph	WS	WD
87101210	15610	28	2.08	7.04	-2.00			13.2	0.50
87101210	15610	18	2.38	6.56					

IDT	JZ	NF	HMO	TP	THp	Dep	wkph	WS	WD
89122313	34885	28	2.44	7.04	30.0			15.90	341.90
89122313	34885	18	2.60	7.11					

IDT	JZ	NF	HMO	TP	THp	Dep	wkph	WS	WD
89122316	34888	28	2.97	7.56	40.0			17.50	344.00
89122316	34888	18	2.93	7.31					

IDT	JZ	NF	HMO	TP	THp	Dep	wkph	WS	WD
89122319	34891	28	3.46	7.56	36.0			19.00	346.20
89122319	34891	18	3.34	7.53					

Mature Sea Sample 1 at 8m and 20m Depth

IDT	JZ	NF	HMO	TP	THp	Dep	wkph	WS	WD
87111107	16327	28	2.05	8.87				10.300	25.400
87111107	16327	18	2.32	8.00					

IDT	JZ	NF	HMO	TP	THp	Dep	wkph	WS	WD
87111110	16330	28	1.95	9.71	16.00			10.600	344.50
87111110	16330	18	2.31	9.85					

IDT	JZ	NF	HMO	TP	THp	Dep	wkph	WS	WD
87111201	16345	28	2.38	10.72	-2.00		0	10.9	233.30
87111201	16345	18	2.73	10.67					

IDT	JZ	NF	HMO	TP	THp	Dep	wkph	WS	WD
89032401	28297	28	2.31	9.71	2.00			6.9	65.00
89032401	28297	18	2.41	9.48					

IDT	JZ	NF	HMO	TP	THp	Dep	wkph	WS	WD
89032404	28300	28	2.21	9.71	10.00			6.1	96.900
89032404	28300	18	2.21	9.48					

IDT	JZ	NF	HMO	TP	THp	Dep	wkph	WS	WD
89032407	28303	28	2.10	9.71	10.00			5.20	128.80
89032407	28303	18	2.12	9.85					

IDT	JZ	NF	HMO	TP	THp	Dep	wkph	WS	WD
89032407	28303	28	2.10	9.71	10.00			5.20	128.80
89032407	28303	18	2.12	9.85					

Mature Sea Sample 2 at 8m and 20m Depth

IDT	JZ	NF	HMO	TP	THp	Dep	wkph	WS	WD
89030704	27892	21	2.31	9.71	18.0			13.2	352.30
89030704	27892	18	2.46	9.14					

IDT	JZ	NF	HMO	TP	THp	Dep	wkph	WS	WD
89030707	27895	21	2.90	9.71	12.00			16.10	354.60
89030707	27895	18	3.11	7.11					

IDT	JZ	NF	HMO	TP	THp	Dep	wkph	WS	WD
89030710	27898	21	3.16	10.72	8			16.3	2.20
89030710	27898	18	3.48	10.24					

IDT	JZ	NF	HMO	TP	THp	Dep	wkph	WS	WD
89030713	27901	21	3.41	10.72	2.00			16.4	9.80
89030713	27901	18	3.77	10.67					

IDT	JZ	NF	HMO	TP	THp	Dep	wkph	WS	WD
89122401	34897	28	3.79	8.87	42.00			18.70	338.50
89122401	34897	18	3.58	8.83					

IDT	JZ	NF	HMO	TP	THp	Dep	wkph	WS	WD
89032407	34903	28	4.27	9.71	22.00			20.00	338.30
89032407	34903	18	2.12	9.48					

IDT	JZ	NF	HMO	TP	THp	Dep	wkph	WS	WD
89032410	34906	28	4.47	10.72	-4.00			19.30	335.60
89032410	34906	18	4.47	9.48					

IDT	JZ	NF	HMO	TP	THp	Dep	wkph	WS	WD
89122413	34909	28	4.68	10.72	18.0			18.5	332.90
89122413	34909	18	5.63	11.13					

Swell Sample 1 at 8m and 20m Depth

IDT	JZ	NF	HMO	TP	THp	Dep	wkph	WS	WD
87031019	10435	28	4.12	13.56	2.00			16.80	3.10
87031019	10435	18	4.49	12.8					

IDT	JZ	NF	HMO	TP	THp	Dep	wkph	WS	WD
87031022	10438	28	4.07	13.56	6.00			15.80	14.90
87031022	10438	18	4.36	12.19					

IDT	JZ	NF	HMO	TP	THp	Dep	wkph	WS	WD
87031101	10441	28	4.00	13.56	-6.00			14.80	26.70
87031101	10441	18	4.22	12.19					

IDT	JZ	NF	HMO	TP	THp	Dep	wkph	WS	WD
89122416	34912	28	4.46	13.56	-18.00			14.10	323.80
89122416	34912	18	4.83	12.8					

IDT	JZ	NF	HMO	TP	THp	Dep	wkph	WS	WD
89122419	34915	28	4.03	13.56	-16.00			9.70	314.70
89122419	34915	18	4.50	12.19					

IDT	JZ	NF	HMO	TP	THp	Dep	wkph	WS	WD
89122501	34921	28	3.71	13.56	-24.00			6.50	291.80
89122501	34921	18	4.00	13.47					

Swell Sample 2 at 8m and 20m Depth

IDT	JZ	NF	HMO	TP	THp	Dep	wkph	WS	WD
89090822	32350	21	1.69	13.56	-18.00			2.60	48.90
89090822	32350	18	1.83	15.06					

IDT	JZ	NF	HMO	TP	THp	Dep	wkph	WS	WD
89090907	32359	21	1.94	13.56	-16.00			0.90	344.50
89090907	32359	18	1.65	13.47					

IDT	JZ	NF	HMO	TP	THp	Dep	wkph	WS	WD
89090910	32362	21	1.94	13.56	-16.00			1.90	28.50
89090910	32362	18	1.65	13.47					

IDT	JZ	NF	HMO	TP	THp	Dep	wkph	WS	WD
89122507	34927	28	2.71	13.56	-22.00			5.20	283.20
89122507	34927	18	2.87	12.80					

IDT	JZ	NF	HMO	TP	THp	Dep	wkph	WS	WD
89122513	34933	28	2.54	13.56	-20.00			3.80	229.10
89122513	34933	18	2.87	12.80					

IDT	JZ	NF	HMO	TP	THp	Dep	wkph	WS	WD
89122519	34939	28	1.96	13.56	-16.00			3.70	163.40
89122519	34939	18	2.16	13.47					

Notes:

**Wind speeds only taken at FRF 625 gauge*

Where,

IDT = date yr mo, day hour

JZ = julian date/time

nf = number of frequencies

hmo = significant wave height

Tp = peak period

thp = direction at spectra peak

dep = depth

wkph = kph

ws = wind speed

wd = wind direction

**Items without a quantity were not provided within the wave spectra data*

VITA

Personal Information

Name: Morgan Menzies Smith

Citizenship: United States

Marital Status: Single

Children: None

Education

- B.S., Civil Engineering, 2015, University of North Florida, Jacksonville, Florida

Association Memberships

- Coasts, Oceans, Ports and Rivers Institute (COPRI)
- American Society of Civil Engineers (ASCE)

Professional Experience

Taylor Engineering, Inc.

- Waterfront Engineer (December 2017-Present)
- Engineering Intern (May 2017- December 2017)

University of North Florida

- Graduate Research Assistant (Fall 2015 – Spring 2018)

HDR, Inc.

- Port Engineering Intern (Summer 2014)